Inorganic Chemistry

ARTICLE

pubs.acs.org/IC

Magnetic Systems with Mixed Carboxylate and Azide Bridges: Slow Relaxation in Co(II) Metamagnet and Spin Frustration in Mn(II) Compound

Yan-Qin Wang,[†] Xiu-Mei Zhang,[†] Xiu-Bing Li,[†] Bing-Wu Wang,[‡] and En-Qing Gao*[,†]

[†]Shanghai Key Laboratory of Green Chemistry and Chemical Processes, Department of Chemistry, East China Normal University, Shanghai 200062, People's Republic of China

[‡]Beijing National Laboratory of Molecular Science, State Key Laboratory of Rare Earth Materials Chemistry and Applications, College of Chemistry and Molecular Engineering, Peking University, Beijing 100871, People's Republic of China

Supporting Information

ABSTRACT: Two coordination polymers formulated as $[\{[Co_2(L)(N_3)_4]\cdot 2DMF\}_n$ (**1**) and $[Mn_2(L)(H_2O)_{0.5}(N_3)_8]_n$ (**2**) (L = 1,4-bis(4-carboxylatopyridinium-1-methyl)-benzene) were synthesized and structurally and magnetically characterized. In compound **1**, the anionic uniform Co(II) chains with mixed (μ-EO-N_3)$_2$(μ-COO) triple bridges (EO = end-on) are cross-linked by the cationic bis(pyridinium) spacers to generate 2D coordination layers. It was demonstrated that the triple bridges mediate ferromagnetic coupling and that the compound represents a new example of the rare systems exhibiting the coexistence of antiferromagnetic ordering, metamagnetism, and slow magnetic dynamics. Compound **2** features the magnetic Δ-chain formed from isosceles triangular units with single μ-EE-N_3 and double (μ-EO-N_3)(μ-COO) bridges (EE = end-to-end). The Δ-chains are interlinked by long organic ligands into a 3D framework with novel net topology and 3-fold interpenetration. The magnetic properties of **2** indicate the presence of spin frustration characteristic of Δ-chains with antiferromagnetic interactions.

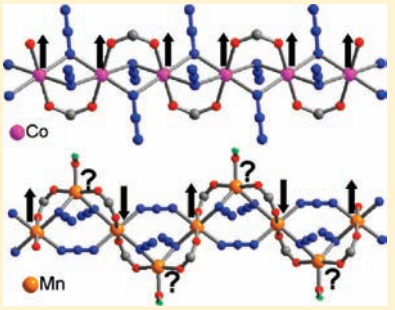

INTRODUCTION

Molecular magnetism is an interdisciplinary field of research that has attracted great attention for decades, with studies focusing on revealing the diverse magnetic phenomena in molecular systems, understanding the underlying physics, and constructing new magnetic materials with potential applications.[1−3] The most extensively studied systems are the metal coordination compounds in which paramagnetic metal ions are linked by short bridging groups into finite-sized polynuclear clusters or 'infinite' coordination polymers. The studies have been much encouraged by the discoveries and establishments of single-molecule magnets (SMMs) and single-chain magnets (SCMs).[3c,4,5] Among the large variety of short bridging groups affording magnetic clusters and polymers, carboxylate and azide have been widely studied owing to their versatility in both structural and magnetic aspects: (i) They can bind two or more metal ions in various bridging modes and can efficiently induce magnetic exchange of different nature and magnitude; and (ii) they can form various coordination systems with different dimensionalities [0D (cluster), 1D (chain), 2D (layer), or 3D] or diverse topologies.[6−9] The rich structural chemistry has afforded rich magnetism, and many molecular magnets with either carboxylate or azide bridges have been synthesized, including different long-range ordered systems,[8c,10] SMMs,[11] and less common, SCMs.[12] The systems containing simultaneous azide and carboxylate bridges also promise diverse magnetic properties, but the known examples are still limited, mostly derived from a few mono- ($RCOO^-$) or dicarboxylate [$R(COO^-)_2$] ligands with neutral R's (methyl, ethyl, phenylene, pyridyl, or pyridyl N-oxide).[13−16] The simultaneous incorporation of the two negatively charged bridges is limited by their competition not only in binding metal ions and but also in compensating the metal charge. To circumvent the charge competition, we have recently explored the use of inner-salt-type (or zwitterionic) carboxylate ligands that bear cationic pyridinium groups to charge compensate the carboxylate groups. Our previous reports have demonstrated that this is an easy and efficient approach toward simultaneously azide- and carboxylate-bridged magnetic networks, including polynuclear clusters, infinite chains and layers, and even 3D frameworks.[17,18] The chain motifs are the most frequently encountered. It has also been demonstrated that simultaneous bridges (double (EO-N_3)(COO), triple (EO-N_3)$_2$(COO), or (EO-N_3)(COO)$_2$; EO = end-on) mediate antiferromagnetic (AF) coupling in Mn(II) species but ferromagneitc (FM) coupling in Co(II) and Ni(II) species.[16b,17,18] The FM coupling in 1D Co(II) systems, combined with the single-ion anisotropy of Co(II), is of particular interest for the design of SCMs. Along this line, we have obtained several systems showing SCM-based magnetic dynamics.[18b,d] The recently reported Co(II) chain

Received: April 9, 2011
Published: June 09, 2011

Chart 1

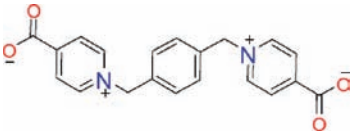

compound with *N*-methylpyridinium-3-carboxylate and with alternating FM pathways $[(EO\text{-}N_3)_2$ and $(EO\text{-}N_3)_2(COO)]$ represents the first SCM with simultaneous azide and carboxylate bridges.[18b]

As a part of systematic study, here we report the structures and magnetic properties of the Co(II) and Mn(II) coordination polymers derived from azide and a long zwitterionic dicarboxylate ligand, 1,4-bis(4-carboxylatopyridinium-1-methyl)benzene (L, Chart 1). The compounds are formulated as $\{[Co_2(L)(N_3)_4]\cdot 2DMF\}_n$ (**1**) and $[Mn^{2}(L)(H_2O)_{0.5}(N_3)_8]_n$ (**2**) and exhibit very different structural features and magnetic properties. Compound **1** contains 2D layers in which uniform Co(II) chains with $(EO\text{-}N_3)_2(COO)$ bridges are interlinked by long organic spacers. In **2**, single EE-N_3 (EE = end-to-end) and double $(EO\text{-}N_3)(COO)$ bridges combine to produce Δ-chains, which are interlinked by long organic ligands into 3D frameworks with novel net topology and with 3-fold interpenetration. The magnetic properties of **1** features the coexistence of intrachain FM coupling, interchain AF ordering, metamagnetism, and slow magnetic dynamics, while **2** behaves as a 1D spin-frustrated system due to the combination of the Δ-chain configuration and intrachain AF interactions.

EXPERIMENTAL SECTION

Materials and Physical Measurements. Elemental analyses were determined on an Elementar Vario ELIII analyzer. The FT-IR spectra were recorded in the range 500−4000 cm^{-1} using KBr pellets on a Nicolet NEXUS 670 spectrophotometer. The phase purity of the bulk or polycrystalline samples was verified by powder X-ray diffraction (PXRD) measurements performed on a Bruker D8-Advance diffractometer equipped with Cu Kα at a scan speed of 1° min^{-1}. Temperature-dependent magnetic measurements were performed on a Quantum Design MPMS-XL5 SQUID magnetometer. The experimental susceptibilities were corrected for the diamagnetism of the constituent atoms (Pascal's tables).

Synthesis. The reagents were obtained from commercial sources and used without further purification, while 1,4-bis(4-carboxylatopyridinium-1-methyl)benzene dihydrobromide ($[H_2L]Br_2$) was prepared according to the literature.[19]

Caution!*. Although not encountered in our experiments, azido compounds of metal ions are potentially explosive. Only a small amount of the materials should be prepared, and it should be handled with care.*

*$\{[Co_2(L)(N_3)_4]\cdot 2DMF\}_n$ (**1**).* A mixture solution of $Co(NO_3)_2\cdot 6H_2O$ (0.0291 g, 0.1 mmol), $[H_2L]Br_2$ (0.0510 g, 0.1 mmol), and sodium azide (0.026 g, 0.4 mmol) in water (1.8 mL) and DMF (0.6 mL) was allowed to stand at room temperature, and red crystals of **1** were obtained in a week. Yield, 30.6% based on L. Anal. calcd for $C_{26}H_{30}Co_2N_{16}O_6$: C, 40.01; H, 3.87; N, 28.71%. Found: C, 39.61; H, 3.78; N, 28.55%. Main IR bands (KBr, cm^{-1}): 2062s [$\nu(N_3)$], 1664s [$\nu_{as}(COO)$], 1622s, 1565 m, 1393s [$\nu_s(COO)$], 1342w, 1293w, 788 m, 660 m.

*$[Mn_2(L)(H_2O)_{0.5}(N_3)_8]_n$ (**2**).* $[H_2L]Br_2$ (0.0510 g, 0.1 mmol) and sodium azide (0.065 g, 1.0 mmol) were dissolved into a mixture of ethanol (2 mL) and water (2 mL), and then the solution was added into the ethanol solution (2 mL) of $Mn(ClO_4)_2\cdot 6H_2O$ (0.0731 g, 0.2 mmol). The mixture was stirred for a few minutes, yielding a little orange-yellow precipitate, which was filtered off. Slow evaporation of the filtrate at room temperature afforded orange-yellow crystals of **2** after one day. The crystals were collected by filtration, washed by water and ethanol, and dried in air. Yield: 85% based on L. Elem anal. calcd (%) for $C_{20}H_{17}Mn_2N_{14}O_{4.5}$: C, 37.81; H, 2.70; N, 30.87%. Found: C, 38.28; H, 3.13; N, 30.69%. Main IR bands (KBr, cm^{-1}): 2073s [$\nu(N_3)$], 2053s [$\nu(N_3)$], 1629s [$\nu_{as}(COO)$], 1568 m, 1456 m, 1393s [$\nu_s(COO)$], 781 m, 690 m.

Table 1. Crystal Data and Structure Refinement for Compounds 1 and 2

compound	**1**	**2**
formula	$C_{26}H_{30}Co_2N_{16}O_6$	$C_{20}H_{17}Mn_2N_{14}O_{4.5}$
Mr	780.52	635.36
crystal system	triclinic	monoclinic
space group	$P\bar{1}$	$C2/c$
a [Å]	6.4671(3)	14.3723(5)
b [Å]	11.7923(6)	23.3952
c [Å]	12.1807(9)	9.8676(4)
β[°]	90.944(2)	129.6550(10)
V(Å^3)	819.41(8)	2554.46(17)
Z	2	4
ρ_{calcd} [g cm^{-3}]	1.582	1.652
μ [mm^{-1}]	1.080	1.049
unique reflections	3308	2641
R_{int}	0.0187	0.0188
R_1 [$I > 2\sigma(I)$]	0.0280	0.0410
wR_2(all data)	0.0837	0.1210

X-ray Crystallography. Diffraction data for **1** and **2** were collected at room temperature on a Bruker Apex II CCD area detector equipped with graphite-monochromated Mo Kα radiation (λ = 0.71073 Å). Empirical absorption corrections were applied using the SADABS program.[20] The structures were solved by the direct method and refined by the full-matrix least-squares method on F^2, with all non-hydrogen atoms refined with anisotropic thermal parameters.[21] All the hydrogen atoms attached to carbon atoms were placed in calculated positions and refined using the riding model, and the water hydrogen atoms in **2** were located from the difference maps. A summary of the crystallographic data, data collection, and refinement parameters for complexes **1** and **2** is provided in Table 1.

RESULTS AND DISCUSSION

Description of the Structures. *Compound **1**.* Compound **1** exhibits 2D coordination networks in which 1D $[Co(N_3)_2(COO)]_n$ chains are interlinked by the zwitterrionic L ligands. The relevant parameters are summarized in Table 2. There are two crystallographically independent Co(II) ions residing at inversion centers, and they both assume the trans-octahedral coordination geometry defined by four equatorial azide nitrogen atoms and two axial carboxylate oxygen atoms (Figure 1, top). The Co−N distances (2.143(2)−2.188(2) Å) are longer than Co−O distances (2.066(1)−2.087(1) Å), indicating an axial elongation of the octahedron. Alternating Co1 and Co2 ions are triply bridged by two EO azides and one syn-syn carboxylate group to generate a uniform chain running along the *a* direction (Figure 1, bottom). The neighboring $[CoN_4O_2]$ octahedra share the edge defined by two bridging nitrogen atoms and inclined with respect to each other, with the dihedral angles between the $[CoN_4]$ equatorial planes being 23.6°. The Co···Co distances spanned by the triple bridge are 3.324(1) Å, and the Co−N−Co

dx.doi.org/10.1021/ic200732f |*Inorg. Chem.* 2011, 50, 6314–6322

Table 2. Selected Distances (Å) and angles (°) for Compound 1[a]

Co1−O2	2.066(1)	Co1−N2	2.182(2)
Co1−N5	2.143(2)	Co2−O1	2.087(1)
Co2−N5	2.161(2)	Co2−N2A	2.188(2)
O2A−Co1-O2	180.0	O2−Co1−N5	87.70(6)
O2−Co1−N5A	92.30(6)	N5A−Co1-N5	180.0
O2A−Co1-N2	89.24(6)	O2−Co1−N2	90.76(6)
N5A−Co1-N2	81.02(6)	N5−Co1−N2	98.98(6)
N2−Co1−N2A	180.0	O1B−Co2−O1	180.0
O1B−Co2−N5	91.76(6)	O1−Co2−N5	88.24(6)
N5−Co2−N5B	180.0	O1−Co2−N2C	90.87(6)
O1−Co2−N2A	89.13(6)	N5−Co2−N2A	80.48(6)
N5−Co2−N2C	99.52(6)	N2A−Co2-N2C	180.00
Co1−N5−Co2	97.40(7)		

[a] Symmetry codes. For **1**: (A) $-x+2, -y, -z+1$; (B) $-x+1, -y, -z+1$; (C) $x-1, y, z$.

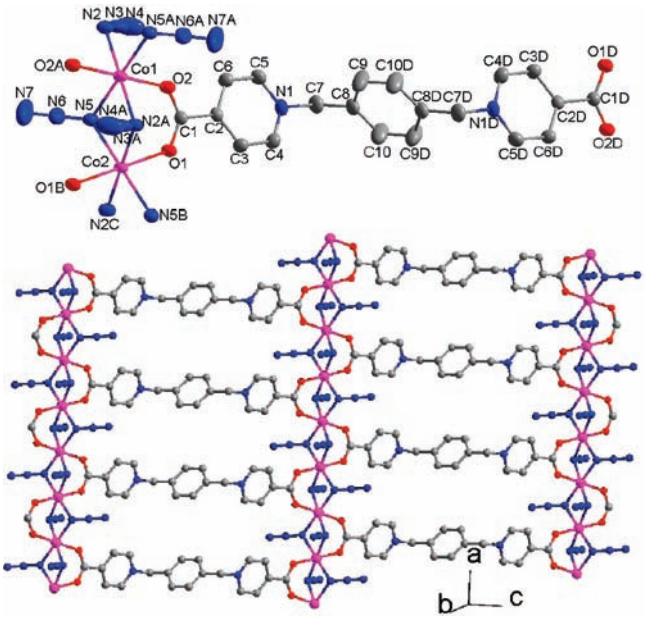

Figure 1. The local coordination environments of the Co centers and the ligands in compound **1**. Hydrogen atoms are omitted for clarity and symmetry codes are: (A) $-x+2, -y, -z+1$; (B) $-x+1, -y, -z+1$; (C) $x-1, y, z$; (D) $2-x, 1-y, -z$ (top) and the 2D network formed by the L ligands connecting the uniform chains with mixed triple bridges (bottom).

angles for the azide bridges are 97.40(7)°. These parameters are comparable to those for previous Co(II) compounds with similar bridges.[13b,18]

The L ligand in the structure is centrosymmetric and adopts the zigzag conformation in which the two 1-menthylpyridinum groups tethered by the 1,4-benzene ring are trans to each other. With each ligand using two syn−syn carboxylate groups to bind two pairs of metal ions from different chains, a stepped 2D layer is formed extending along the (011) plane. The nearest interchain Co···Co distances within the layer are 19.69(4) Å. The layers are packed in parallel with weak interlayer hydrogen bonds, which involve C−H groups from one layer and terminal azide

Table 3. Selected Distances (Å) and Angles (°) for Compound 2[a]

Mn1−O3	1.968(7)	Mn1−O1	2.122(2)
Mn1−N4	2.166(2)	Mn1−N1	2.394(6)
Mn2−O2	2.174(2)	Mn2−N7	2.204(3)
Mn2−N4	2.274(2)	O3−Mn1−O1	86.43(6)
O1A−Mn1-O1	172.85(11)	O3−Mn1−N4A	126.14(6)
O1−Mn1−N4	92.63(8)	O1−Mn1−N4A	91.58(8)
O3−Mn1−N4	126.14(6)	O1A−Mn1-N4	91.58(8)
N4A−Mn1-N4	107.72(13)	O3−Mn1−N1	36.5(2)
O1A−Mn1-N1	85.0(2)	O1−Mn1−N1	89.2(2)
N4A−Mn1-N1	162.6(2)	N4−Mn1−N1	89.6(2)
N4−Mn1−N1A	162.6(2)	O1A−Mn1-N1A	89.2(2)
N1−Mn1−N1A	73.1(4)	O2C−Mn2−O2	180.0
O2C−Mn2−N7	89.29(2)	O2−Mn2−N7	90.71(2)
N7−Mn2−N7C	180.00	O2C−Mn2−N4	84.02(8)
O2−Mn2−N4	95.98(8)	N7−Mn2−N4	91.45(10)
N7C−Mn2−N4	88.55(10)	O2−Mn2−N4C	84.02(8)
N7C−Mn2−N4C	91.45(1)	N4−Mn2−N4C	180.0
Mn1−N4−Mn2	119.38(9)		

[a] Symmetry codes: A: $x, -y, z-0.5$; B: $x+1, -y, z+0.5$; C: $x+0.5, y-0.5, z$.

nitrogen atoms from another layer. The offset packing of the stepped layers generates interlayer channels along the chain direction, which are filled by lattice DMF molecules that are associated to the layers via weak C−H···O and C−H···N hydrogen bonds (see the Supporting Information, Figure S1). The nearest interlayer Co···Co distance is 11.792(1) Å.

Compound ***2***. Single-crystal X-ray analysis on **2** revealed a 3D framework consisting of 1D anionic polymeric chains based on triangle $[Mn_3(N_3)_3(COO)_2(H_2O)]$ subunits. The relevant parameters are summarized in Table 3. As shown in Figure 2a, there are two crystallographically independent Mn(II) atoms. The Mn2 atom is located at an inversion center and assumes a trans-octahedral $[N_4O_2]$ coordination geometry completed by four equatorial azide nitrogen atoms (N4, N4C, N7, and N7C, Mn−N = 2.274(2) and 2.204(3) Å) and two axial carboxylate oxygen atoms (O2 and O2C, Mn−O = 2.174(2) Å). Mn1 resides on a crystallographic C_2 axis with a disordered coordination environment. Each Mn1 is ligated by two cis azide nitrogen atoms (N4 and N4A) in equatorial positions and two carboxylate oxygen atoms (O1 and O1A) in axial positions. The coordination geometry can be either distorted octahedral with another two equatorial azide ligands (N1 and N1A, both having an occupancy of 0.5), or trigonal bipyramidal with an equatorial aqua ligand (O3, also with an occupancy of 0.5). Mn1 and Mn2 atoms are doubly linked by an azide bridge (N4) in the EO mode and a carboxylate bridge (O1−C1−O2) in the syn−syn mode, with Mn1−N4−Mn2 = 119.4(9)° and Mn···Mn = 3.834(5) Å, and two C_2-symmetry related Mn2 atoms linked to the same Mn1 atom are singly linked by an azide bridge in the EE (end-to-end) mode, with Mn2−N7C−N8C = 130.3(3)°, Mn2−N7C−N8C−N7D−Mn2A = 71.4(4)°, and Mn···Mn = 5.544(2) Å. Thus a Mn1 and two Mn2 atoms are linked into a isosceles triangle $[Mn_3(N_3)_3(COO)_2]$. The alternating up- and downward triangular subunits share the Mn2 atoms to generate an infinite 'Δ-chain' with all Mn2's being collinear along the *c* direction (Figure 2b).

dx.doi.org/10.1021/ic200732f |*Inorg. Chem.* 2011, 50, 6314–6322

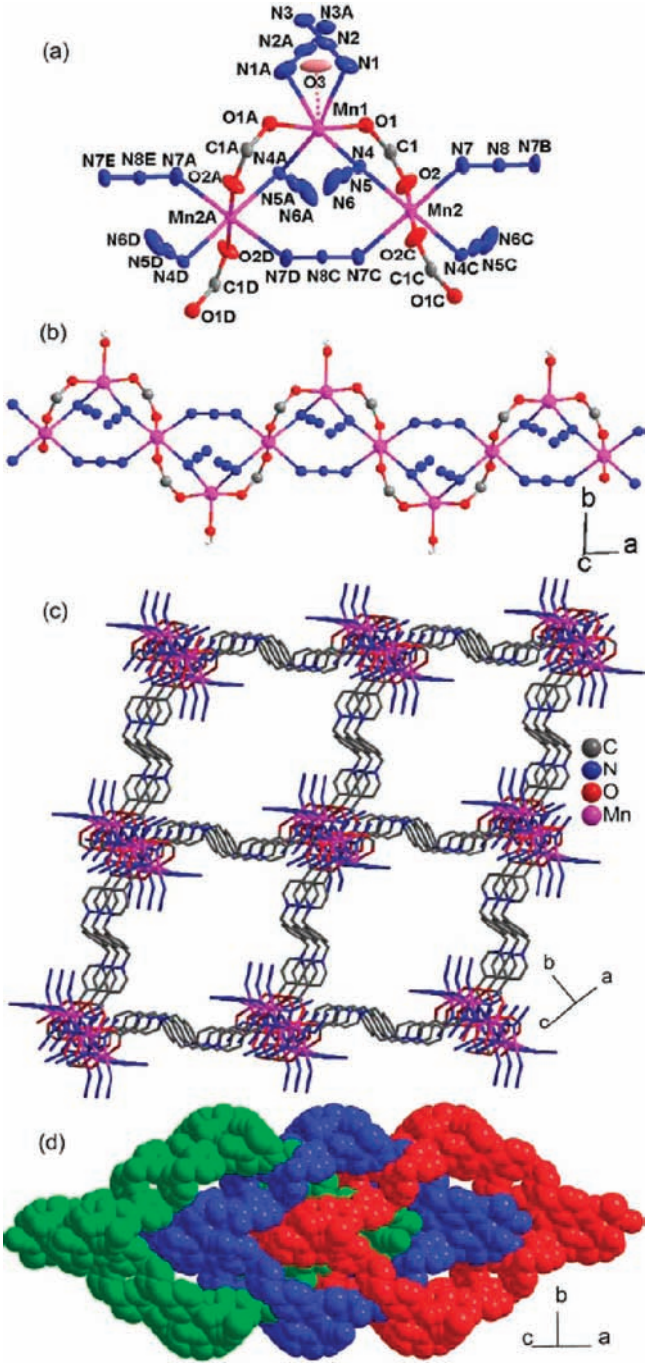

Figure 2. (a) Triangular unit in compound **2**. The disorder of the Mn environment is shown (see the text). Hydrogen atoms are omitted for clarity and symmetry codes are: (A) $x, -y, z - 0.5$; (B) $x + 1, -y, z + 0.5$; (C) $x + 0.5, y - 0.5, z$; (D) $-0.5 - x, -0.5 + y, -z - 0.5$; (E) $-1 - x, -y, -1 - z$. (b) 1D chain along the (101) direction (the disordered azide ions are omitted for clarity). (c) A single 3D network. (d) The three-fold interpenetration of the networks.

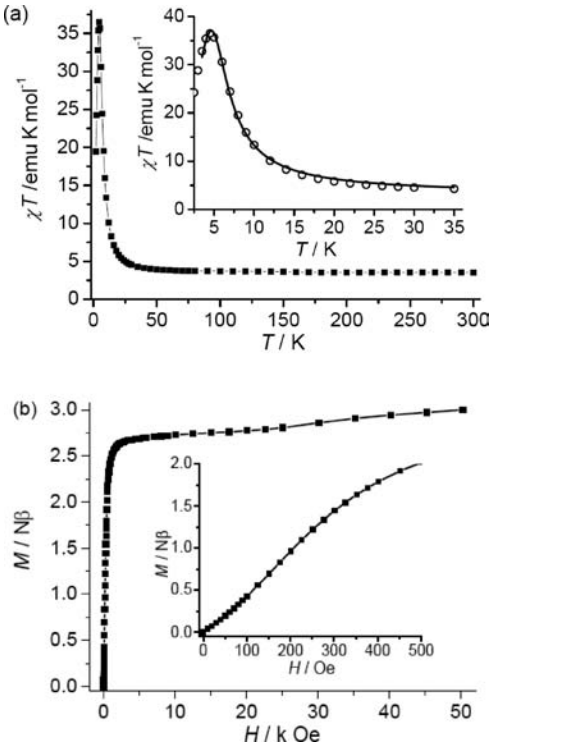

Figure 3. (a) χT versus T plot of **1** at 1 kOe. Inset: a blow-up of the plot in the low-temperature region with the best-fit line to Ising model [eq 1 in the text]. (b) Isothermal magnetization at 2 K. Inset: a blow-up of the curve in the low-field region.

The L ligand in **2** has the same symmetry, conformation, and coordination mode as that in **1**. Each Δ-chain is linked to four identical chains through L ligands in four different orientations to give a complicated 3D network (Figure 2c). A convenient way of simplifying the 3D network is to assume the dicarboxylate L ligand as a building block in which two Y-shaped moieties are connected in a tail-to-tail fashion. Thus the carboxylate C atom acts as a three-connected node, and then the metal ions are four- or six-connected: Each Mn1 is connected to two $C_{carboxylate}$ atoms and two Mn2's (through EO azides), and each Mn2 is connected to two $C_{carboxylate}$ atoms, two Mn1's (through EO azides), and two Mn2's (through EE azides). In this way, the 3D network is reduced to a 3,4,6-connected trinodal net with Schläfli symbol $(3 \times 10^2)_2(3^3 \cdot 4^2 \cdot 5)(3^4 \cdot 4^2 \cdot 10^5 \cdot 11^3 \cdot 12)$ (Supporting Information, Figures S2 and S3), according to the topological analysis using the TOPOS program.[22] This represents a new topology which has not yet been recognized before.

The single network has very large "empty" space related to the long interchain linkers (Figure 2c). Thus three equivalent 3D networks interpenetrate with one another to fill the space (Figure 2d). The interpenetration is sustained by the O−H···N hydrogen bonds involving the coordinated water and the terminal azide ligands from different nets (Supporting Information, Figure S4). Via the hydrogen bonds, each Mn1 from one net is linked to two Mn1's from the other two nets. Taking the hydrogen bonds as additional connections, Mn1 becomes a 6-connected node, and the three interpenetrated coordination nets can be viewed as a single 3,6,6-connected trinodal net with Schläfli symbol $(3 \cdot 8^2)_2(3^3 \cdot 4^2 \cdot 5 \cdot 8^9)(3^4 \cdot 4^2 \cdot 8^5 \cdot 9^3 \cdot 10)$ (Supporting Information, Figure S5). This topology is also unprecedented.

Magnetic Properties. *Complex* ***1***. The magnetic susceptibility (χ) of compound **1** was measured under 1 kOe in the 2−300 K range. The χT value per Co(II) at room temperature is 3.52 emu mol^{-1} K, falling within the usual range for octahedral Co(II) in the $^4T_{2g}$ state. As the temperature is lowered, χT increases to maxima of 36.50 emu K mol^{-1} at 4.5 K and then

dx.doi.org/10.1021/ic200732f |*Inorg. Chem.* 2011, 50, 6314–6322

drops rapidly upon further cooling (Figure 3a). The $1/\chi$ vs T plot above 45 K obeys the Curie−Weiss law with C = 3.43 emu mol^{-1} K and θ = 7.31 K. The increase of χT with decreased temperature clearly indicates FM interactions mediated through the mixed (μ-EO-N_3)$_2$(μ-COO) triple bridges. The appearance of the χT maximum at low temperature may arise from: (i) the saturation effect induced by the applied magnetic field, (ii) interchain AF interactions, and (iii) the finite-chain effect that operates when the divergence of the correlation length along the chain is suppressed by naturally occurring defects. The last effect itself leads to a saturation (not a decrease) of χT at low temperature, but its combination with AF interactions between finite-chain segments can lead to a decrease in χT.

Owing to the metamagnetic properties of **1** (see below), the interchain AF interactions are overcome in the field of 1 kOe, and the observed χT maximum should be mainly due to a field-induced effect. At low temperature, the Co(II) system can be handled as an Ising chain of effective S = 1/2 spins. Based on the Hamiltonian $\boldsymbol{H} = -2J\Sigma \boldsymbol{S}_{i,z}\boldsymbol{S}_{i+1,z}$, the parallel susceptibility under a finite field H is[5b,c]

$$\chi_{//} = M_{//}/H = (Ng_{//}S\mu_B/H)\sinh(g_{//}S\mu_B H/kT) / [\sinh^2(g_{//}S\mu_B H/kT) + \exp(-8JS^2/kT)]^{1/2} \quad (1)$$

Neglecting the perpendicular component (much smaller than the parallel one in low field) and applying $\chi = \chi_{//}/3$ for polycrystalline data, the expression was used to fit the susceptibility data between 3.5−35 K (the fit was not extended to lower temperature due to the presence of long-range ordering, see below). The best fit reproduces the χT maximum with J = 10.6 cm^{-1} and $g_{//}$ = 9.78, indicating the 1D correlation character of the system above 3.5 K. The positive value of J confirms the FM nature of the interactions through triple (μ-EO-N_3)$_2$(μ-COO) bridges, which is consistent with that found for previous Co(II) compounds with similar bridging motifs.[13b,18] The $g_{//}$ value corresponds to an effective Curie constant $C_{eff} = N\mu_B{}^2 g_{//}{}^2 S^2/3k$ = 2.97 emu mol^{-1} K, which is consistent with Co(II) with significant orbital momentum. The difference between C_{eff} and the constant (3.43 emu mol^{-1} K) obtained from the Curie−Weiss law is not surprising considering the complicacy of Co(II) magnetism, the different approximation levels, and the different temperature ranges used to estimate the parameters.

To estimate the interchain AF interactions and the possible finite-chain effect, ac χ' data under zero dc field in the temperature range 3.5−20 K have been used (Supporting Information, Figure S6). A simple approach is to assume a pseudo-1D model,[24] which is characterized by strong coupling along infinite chains and weak coupling between the chains. With the Ising model, the zero-field susceptibility for the infinite chain is[23]

$$\chi_{//,\infty} = (N\mu_B{}^2 g_{//}{}^2 S^2/kT)\exp(4JS^2/kT) \quad (2)$$

In the mean-field approximation, the susceptibility of the system in which each chain is weakly coupled with z chains is[24]

$$\chi_{//} = \chi_{//,\infty}/[1 - 2zJ'\chi_{//,\infty}/(N\mu_B{}^2 g_{//}{}^2)] \quad (3)$$

The best fit using the above expressions and $\chi = \chi_{//}/3$ reproduces the χT maximum of the ac data with J = 13.7 cm^{-1}, zJ' = −0.16 cm^{-1}, and $g_{//}$ = 10.4. The J parameter is in fair agreement with that obtained previously.

An alternative approach is taking into account the finite-chain effect. Assuming an "monodisperse" approximation for the chain length (all the chain segments contain n magnetic sites), the low-temperature susceptibility per site has been deduced as[5c,25]

$$\chi_{//,n} = \chi_{//,\infty}\{1 - [1 - \exp(-A)]/A\} \quad (4)$$

Where $A = 2n\exp(-4JS^2/kT)$. This expression predicts a saturation of $\chi_{//,n}T = nN\mu_B{}^2 g_{//}{}^2 S^2/k$ at low temperature. To account for the decrease of χT at low temperature, AF interactions between the finite chains should be considered. A model assuming that the chain segments are AF coupled across the defects was proposed by Coulon et al. to account for the weak χT decrease of a Mn_2Ni chain system.[26] The system was treated as a chain of segments with intrasegment F coupling and intersegment AF coupling, neglecting interchain AF interactions. This model should not be suitable for our compound, where the occurrence of AF ordering indicates the importance of interchain interactions. Differently, we have attempted to fit the χ' data in the mean-field approximation (replacing $\chi_{//,\infty}$ in eq 3 for $\chi_{//,n}$). The best fit led to n = 240 (or chain length $L \approx$ 80 nm) with the other parameters (J = 13.7 cm^{-1}, zJ' = −0.15 cm^{-1}, and $g_{//}$ = 10.5) similar to those from the infinite model. However, it must be noted that the fit is actually insensitive to the variation of n, all the fits with n fixed in the range from ca. 120 to infinite could lead to reasonable agreement (the other parameters show only minor variations). So the presence of finite-chain effect could not be determined unambiguously from the fits.

Isothermal magnetization of **1** measured at 2 K (Figure 3b) shows an overall rapid rise as the field is lifted from zero, confirming the intrachain interaction. The magnetization shows a slow increase in the high-field region with no indication of saturation even at 5 T, indicating magnetic anisotropy.[5,27] Note that there is a slow step around 3 T, which appears as a weak maximum in the $dM/dH - H$ plot (Supporting Information, Figure S7 inset). Stepped magnetization observed in a few SCM systems has been attributed to noncollinearity of local anisotropy axes.[5a,12a] For instance, the magnetization steps for the Co-PhOMe SCM material consisting of Co(II)-radical ferrimagnetic chains[5a] have been theoretically related to the helical tilting of the local anisotropy axes of Co(II) ions.[28] The magnetization step observed in **1** is consistent with the structural feature that the neighboring [CoN_4O_2] polyhedrons inclined with respect to each other (vide supra), which indicates noncollinearity of local anisotropy axes.

A blow-up of the $M-H$ curve in the very low-field region shows a sigmoid shape (Figure 3b, inset), as evidenced by a sharp maximum at 175 Oe in the $dM/dH - H$ plot (Supporting Information, Figure S7). The Zeeman energy in this weak field is too low to be associated with noncollinearity of local anisotropy axes along the chain. Instead, this low-field step may suggest field-induced metamagnetism related to interchain interactions: The FM chains in **1** are ordered at zero field by interchain AF interactions, and the AF order can be broken up by applying an external field above the critical value of H_C =175 Oe. The interchain interaction can be roughly related to H_C in the mean-field approximation:[29]

$$g_{//}\mu_B S H_C = 2|zJ'|S^2$$

Assuming $g_{//} \approx 10$ with S = 1/2, $|zJ'|$ is estimated to be about 0.082 cm^{-1}. This value is in fair agreement with that estimated from the susceptibility data.

dx.doi.org/10.1021/ic200732f |Inorg. Chem. 2011, 50, 6314–6322

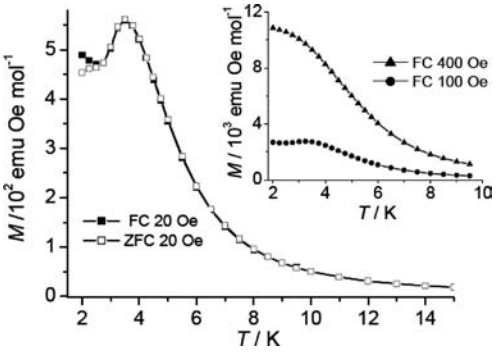

Figure 4. ZFC and FC magnetization curves of **1** at 20 Oe. Inset: FC magnetization curves at 100 and 400 Oe.

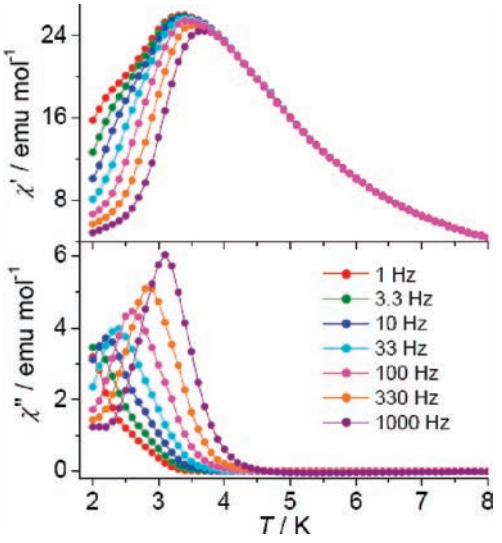

Figure 5. $\chi'(T)$ and $\chi''(T)$ plots for **1** at frequencies 1−1000 Hz (from left to right) with H_{dc} = 0 and H_{ac} = 3.5 Oe.

The sigmoid shape is also displayed by the hysteresis loop measured at 2 K (Supporting Information, Figure S8). The hysteresis loop revealed negligible coercive field and remnant magnetization, indicating the soft-magnet characteristics of **1**. The metamagnetism is also confirmed by field-cooled (FC) measurements under different fields. The FC magnetization under 20 Oe (Figure 4) shows a maximum at about 3.5 K, supporting the occurrence of AF ordering. When the external field is increased (Figure 4, inset), the maximum shifts toward low temperature (see the 100 Oe FC curve in Figure 4) and finally disappears (see the 400 Oe FC curve), confirming the field-induced transition from AF to FM states.

The zero-field-cooled (ZFC) magnetization at 20 Oe is also measured (Figure 4), which shows evident divergence from the FC magnetization below 2.8 K. The thermal irreversibility is rather unusual for an AF-ordered phase.

Thermal ac susceptibility measurements (Figure 5) were performed on **1** under a zero dc field to gain insight into the magnetic behaviors. The compound exhibits not only in-phase ac susceptibility (χ') but also out-of-phase signals (χ''), which is atypical of normal antiferromagnets. The ac susceptibilities are frequency dependent. The frequency dependence can be measured by the φ parameter defined by $\varphi = (\Delta T_p/T_p)/\Delta(\log f)$,

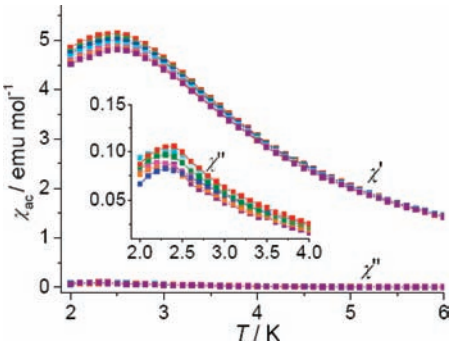

Figure 6. Ac susceptibilities of **1** measured at frequencies 1, 3.3, 10, 33, 100, 330, and 1000 Hz under dc field of 400 Oe with a driving ac field of 3.5 Oe. Inset: the details of the $\chi''(T)$ plots at temperature between 2 and 4 K.

where T_p is the peak temperature of the $\chi''(T)$ plot at a certain frequency (f).[30] For **1**, φ was estimated to be 0.15, which is out of the usual range for spin glasses but consistent with superparamagnets including SCMs ($0.1 \leq \varphi \leq 0.3$).[30,31] Furthermore, the relaxation time $\tau(T)$ data derived from the $\chi''(T)$ peaks follows the Arrhenius law $\tau = \tau_o \exp(\Delta_\tau/T)$ (Supporting Information, Figure S9) with $\tau_o = 2.3 \times 10^{-9}$ s and Δ_τ = 34.8 K, suggesting a thermally activated relaxation with an energy barrier. The Δ_τ and τ_o values lie in the usual range for superparamagnets including SCMs but atypical of canonical spin glasses.[5e,31] For spin glasses, the relaxation process involves much more than simple thermal activation, and the fitting to the Arrhenius law usually yields physically unrealistic Δ_τ and τ_o values.[31,32] The isothermal ac measurements in the frequency range 0.1−1000 Hz produced a semicircle $\chi''-\chi'$ plot (Cole−Cole diagram) at 2.4 K for **1** (Supporting Information, Figure S10). The data were fitted to the generalized Debye model[33] and gave an α parameter of 0.37, which lies in the range for reported SCMs[5e] and suggests a distribution of relaxation time.

Thus, considering that the compound contains ferromagnetic and anisotropic chains, the ac magnetic measurements seem to indicate a SCM-based dynamic behavior. In this assumption, the slow dynamics is intrinsic to a single chain, and the activation energy of magnetization relaxation arises from magnetic exchange and anisotropy within the chain. This assumption does not contradict the AF order observed at zero field, because it has recently been demonstrated, both theoretically and experimentally,[18c,24b,27b,34] that AF order does not necessarily suppress slow dynamics of the SCM components of the materials.

However, the SCM assumption is not supported by the thermal ac measurements under a static field (Figure 6). The measurements were performed under 400 Oe, a field above the critical field for the metamagnetic transition, and thus the ac susceptibilities are for the field-induced ferromagnetic phase. As expected, the ac signals in the dc field are significantly reduced in amplitude when compared to those observed in the zero dc field, because the material in dc field is less responsive to ac field.[35] The in- and out-of-phase components exhibit maxima at about 2.5 and 2.3 K, respectively, and both maximum positions show no evident dependence on frequency, suggesting the absence of slow relaxation dynamics in the frequency range measured.

The effects of external magnetic field on the SCM dynamics of a few $Mn^{III}Ni^{II}$ and $Mn^{III}Fe^{III}$ systems have been theoretically and experimentally studied by Coulon and co-workers.[34,36]

dx.doi.org/10.1021/ic200732f |*Inorg. Chem.* 2011, 50, 6314–6322

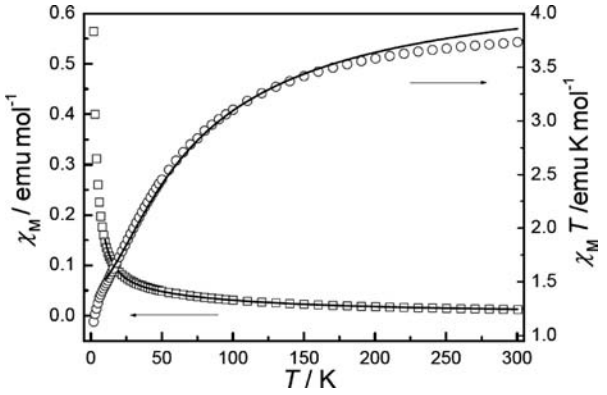

Figure 7. Temperature dependence of χ and χT for **2** at 1 kOe applied field. The solid lines are the best fit (see text).

Chart 2

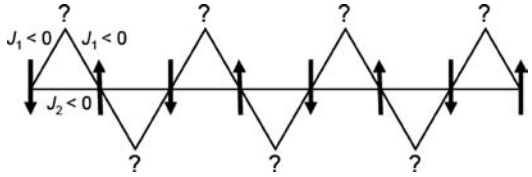

A combined experimental and theoretical study demonstrated that the relaxation time of SCMs can be reduced by external fields because the dynamics of an ferromagnetic Ising chain and that of an magnetic unit are both frequency dependent.[36] However, for an $Mn^{III}Ni^{II}$ SCM in the AF ordered phase, it has been demonstrated that the relaxation time can be enhanced by external fields, with a maximum close to the metamagnetic transition field.[34] Thus, the SCM dynamics can be modified by external fields, but complete suppression is unlikely.

Therefore, the slow dynamics of **1** observed in zero static field is unlikely intrinsic to single chains. Phenomenologically, the slow dynamics is associated with the AF order of the chains because it is "suppressed" in the field-induced FM phase. The origin or mechanism of the phenomenon is open to further investigations, in both experimental and theoretical aspects.

Complex **2**. The χT value per Mn for this compound at 300 K is about 3.73 emu mol^{-1} K, lower than the spin-only value (4.38 emu mol^{-1} K) expected for one magnetic isolated high-spin Mn(II) ions. As the temperature is lowered to 2 K, χ value increases, but the product decreases (Figure 7). The data above 38 K follow the Curie−Weiss law with C = 4.19 emu K mol^{-1} and θ = −34.8 K. The C value corresponds to g = 1.97, and the large negative θ value suggests AF interactions between Mn(II) ions.

Neglecting the interactions through the long organic spacers and the weak hydrogen bonds between the Δ-chains, there are two types of intrachain superexchange pathways corresponding to different bridging motifs (Figure 2b and Chart 2): J_1 through the mixed (μ-EO-N_3)(μ-COO) double bridge defining the side of the isosceles triangle, and J_2 through the single EE azide bridge defining the base. In order to evaluate the exchange, the magnetic data are fitted by least-squares fitting procedure with the Levenberg−Marquardt algorithm using the program MAGPACK.[37] The fit was performed using a seven-membered ring model. The best-fit parameters in the temperature range of 10−300 K are J_1 = −1.74 cm^{-1}, J_2 = −3.26 cm^{-1}, and g = 2.00.

The fitted parameters suggest that both the double and single bridges mediate AF interactions between Mn(II) ions, with the values lying in the usual ranges for such bridges. We note that all the known Mn(II) complexes with simultaneous azide and carboxylate bridges exhibit AF interactions, whether the bridges are double or triple [(μ-EO-N_3)$_2$(μ-COO) and (μ-EO-N_3)(μ-COO)$_2$].[16b,17,18] The (μ-EO-N_3)(μ-COO) double bridges have been observed in a few Mn(II) compounds, with similar Mn−N−Mn angles (∼120°) and similar interaction parameters (−1.5 to −2.5 cm^{-1}).[16a,b] The EE bridge is very common in metal azide compounds, and in the known Mn(II) compounds it always induces antiferromagnetic interactions in the magnitude of several cm^{-1}.[6a,7c,7g,38]

A Δ-chain with similar AF exchange parameters for the triangular unit provides a good example of 1D spin frustration (Chart 2). Although the Δ-chain topology has been of great theoretical and experimental interest for the study of 1D spin frustration,[39] real examples of Mn(II) species are still very rare. A previous example is the Mn(II) complex with 1,2-cyclohexanediamine-*NNN′N′*-tetraacetate (CDTA), in which Mn(II) ions are bridged into Δ-chains by carboxylate groups.[39a] However, in contrast to the isosceles triangle in **2**, the triangle unit in the Mn−CDTA chain has three different edges (μ_2-O, syn−anti and, anti−anti carboxylate), corresponding to three J parameters in the range −1.1 to −0.23 K.

Spin frustration tends to suppress or significantly reduce short- and long-range magnetic order.[39,40] In 1−3D AF Mn(II) systems without spin frustration, the susceptibility exhibits a maximum at nonzero temperature. The effect of spin frustration in the isosceles Δ-chain model has been analyzed by Borrás-Almenar et al.[39a] 1D uniform Mn(II) chain with only nearest-neighboring AF coupling (J), which is related to the isosceles Δ-chain with J_2 = 0 (Chart 2), displays a characteristic χ maximum at $T \approx |J|/2k$, indicative of short-range AF order along the chain. When next-nearest-neighboring AF coupling ($J_2 < 0$) is introduced, the characteristic maximum is broadened toward lower temperature and become less and less pronounced as the ratio J_2/J_1 is increased. According to Borrás-Almenar et al, when $J_2/J_1 \geq 0.5$, the maximum disappears and a continuous increase of χ is observed upon cooling, indicating the destruction of the 1D AF order by spin frustration. In **2**, the ratio is about 1.9, and no maximum was observed in the χ versus T plot down to 2 K, indicating the operation of spin frustration.

Thermal ac susceptibility measurements (Supporting Information, Figure S11) were performed on **2** under zero dc field to detect the possible dynamic behaviors related to spin frustration. The χ' component is characterized by a continuous increase upon cooling, as observed for the dc susceptibility. No frequency dependence and no out-of-phase signal were observed, indicating the absence of slow dynamics. This is not surprising considering the 1D character of spin frustration and the isotropic nature of Mn(II).

■ CONCLUSION

The structures and magnetic properties of the Co(II) and Mn(II) compounds with azide and zwitterionic 1,4-bis(4-carboxylatopyridinium-1-methyl)benzene ligand have been described. In compound **1**, the anionic uniform Co(II) chains with mixed (μ-EO-N_3)$_2$(μ-COO) triple bridges are cross-linked by the cationic bis(pyridinium) spacers to generate 2D coordination layers. It has been demonstrated that the triple bridges

mediate FM coupling and that the compound represents a new example of the rare systems exhibiting the coexistence of AF ordering, metamagnetism, and slow magnetic dynamics. Compound **2** features the magnetic Δ-chain formed from isosceles triangular units with single μ-EE-N_3 and double (μ-EO-N_3)(μ-COO) bridges. The Δ-chains are interlinked by long organic ligands into a 3D framework with novel net topology. The framework displays three-fold interpenetration sustained by hydrogen bonds. The magnetic properties of **2** indicate the presence of spin frustration, which is intrinsic to Δ-chains with comparable and competing AF interactions. This work, in continuation with our previous reports, further demonstrates the great potential of generating materials with novel structural and magnetic features by using the mixed azide and zwitterionic carboxylate approach.[17,18]

■ ASSOCIATED CONTENT

Supporting Information. Crystallographic information for compounds **1** and **2** in CIF format and supplementary structural graphics are available. This material is available free of charge via the Internet at http://pubs.acs.org.

■ AUTHOR INFORMATION

Corresponding Author
*E-mail: eqgao@chem.ecnu.edu.cn.

■ ACKNOWLEDGMENT

This work is supported by NSFC (91022017) and the Fundamental Research Funds for the Central Universities. We are thankful to Professor Song Gao (Peking University) for his help in magnetic discussion.

■ REFERENCES

(1) (a) Gatteschi, D.; Kahn, O.; Miller, J.-S.; Palacio, F. *Magnetic Molecular Materials*; KluwerAcademic: Dordrecht, The Netherland, 1991. (b) Kahn, O. *Molecular Magnetism*; VCH: New York, 1993.

(2) (a) Miller, J.-S.; Epstein, A.-J. *Angew. Chem., Int. Ed. Engl.* **1994**, *33*, 385. (b) *Molecular Magnetism: from Molecular Assemblies to Devices*; Coronado, E., Delhaes, P., Gatteschi, D., Miller, J.-S., Eds.; NATO ASI Series 15; Kluwer: Dordrecht, The Netherland, 1995.

(3) (a) Miller, J.-S. *Adv. Mater.* **2002**, *14*, 1105. (b) *Magnetism: Molecules to Materials*; Miller, J.-S., Drilon, M., Eds.; Willey-VCH: Weinheim, Germany, 2002−2005; Vol. I−V. (c) Gatteschi, D.; Sessoli, R. *Angew. Chem., Int. Ed.* **2003**, *42*, 268.

(4) (a) Oshio, H.; Nihei, M.; Koizumi, S.; Shiga, T.; Nojiri, H.; Nakano, M.; Shirakawa, N.; Akatsu, M. *J. Am. Chem. Soc.* **2005**, *127*, 4568. (b) Burgert, M.; Voss, S.; Herr, S.; Fonin, M.; Groth, U.; Rüdiger, U. *J. Am. Chem. Soc.* **2007**, *129*, 14362. (c) Wu, Q.; Li, Y.-G.; Wang, Y.-H.; Clérac, R.; Lu, Y.; Wang, E.-B. *Chem. Commun.* **2009**, 5743. (d) Xu, G.-F.; Wang, Q.-L.; Gamez, P.; Ma, Y.; Clérac, R.; Tang, J.- K.; Yan, S.- P.; Cheng, P.; Liao, D.- Z. *Chem. Commun.* **2010**, *46*, 1506.

(5) (a) Caneschi, A.; Gatteschi, D.; Lalioti, N.; Sangregorio, C.; Sessoli, R.; Venturi, G.; Vindigni, A.; Rettori, A.; Pini, M. G.; Novak, M. A. *Angew. Chem., Int. Ed.* **2001**, *40*, 1760. (b) Clérac, R.; Miyasaka, H.; Yamashita, M.; Coulon, C. *J. Am. Chem. Soc.* **2002**, *124*, 12837. (c) Coulon, C.; Miyasaka, H.; Clérac, R. *Struct. Bonding (Berlin)* **2006**, *122*, 163. (d) Bogani, L.; Vindigni, A.; Sessoli, R.; Gatteschi, D. *J. Mater. Chem.* **2008**, *18*, 4750. (e) Sun, H.-L.; Wang, Z.- M.; Gao, S. *Coord. Chem. Rev.*, **2010**, *254*, 1081 and references therein.

(6) (a) Ribas, J.; Escuer, A.; Monfort, M.; Vicente, R.; Cortés, R.; Lezama, L.; Rojo, T. *Coord. Chem. Rev.* **1999**, *193*, 1027. (b) Escuer, A.; Aromí, G. *Eur. J. Inorg. Chem.* **2006**, *23*, 4721. (c) Wang, X.-Y.; Wang, Z.-M.; Gao, S. *Chem. Commun.* **2008**, 3, 281. (d) Gao, E.-Q.; Wang, Z.-M.; Yan, C.-H. *Chem. Commun.* **2003**, 1748.

(7) (a) Ge, C.-H.; Cui, A.-L.; Ni, Z.-H.; Jiang, Y.-B.; Zhang, L.-F.; Ribas, J.; Kou, H.-Z. *Inorg. Chem.* **2006**, *45*, 4883. (b) Das, A.; Rosair, G. M.; Salah El Fallah, M.; Ribas, J.; Mitra, S. *Inorg. Chem.* **2006**, *45*, 3301. (c) Gao, E.-Q.; Bai, S.-Q.; Yue, Y.-F.; Wang, Z.-M.; Yan, C.-H. *Inorg. Chem.* **2003**, *42*, 3642. (d) Escuer, A.; Mautner, F. A.; Goher, M. A. S.; Abu-Youssef, M. A. M.; Vicente, R. *Chem. Commun.* **2005**, 605. (e) Gao, E.-Q.; Yue, Y.-F.; Bai, S.-Q.; He, Z.; Yan, C.-H. *J. Am. Chem. Soc.* **2004**, *126*, 1419. (f) Wang, X.-Y.; Wang, L.; Wang, Z.-M.; Gao, Song. *J. Am. Chem. Soc.* **2006**, *128*, 674. (g) Gao, E.-Q.; Cheng, A.-L.; Xu, Y.-X.; He, M.-Y.; Yan, C.-H. *Inorg. Chem.* **2005**, *44*, 8822.

(8) (a) Kurmoo, M. *Chem. Soc. Rev.* **2009**, *38*, 1353. (b) Gavrilenko, K. S.; Punin, S. V.; Cador, O.; Golhen, S.; Ouahab, L.; Pavlishchuk, V. V. *Inorg. Chem.* **2005**, *44*, 5903. (c) Zheng, Y.-Z.; Xue, W.; Zheng, S.-L.; Tong, M.-L.; Chen, X.-M. *Adv. Mater.* **2008**, *20*, 1534. (d) Huang, Y.-G.; Yuan, D.-Q.; Pan, L.; Jiang, F.-L.; Wu, M.-Y.; Zhang, X.-D.; Wei, W.; Gao, Q.; Lee, J. Y.; Li, J.; Hong, M.-C. *Inorg. Chem.* **2007**, *46*, 9609.

(9) (a) Biswas, C.; Mukherjee, P.; Drew, M. G. B.; Gómez-García, C. J.; Clemente-Juan, J. M.; Ghosh, A. *Inorg. Chem.* **2007**, *46*, 10771. (b) Li, M.-Y.; Ako, A. M.; Lan, Y.-H.; Wernsdorfer, W.; Buth, G.; Anson, C. E.; Powell, A. K.; Wang, Z.-M.; Gao, S. *Dalton Trans.* **2010**, *39*, 3375. (c) Han, Z.-B.; Ji, J.-W.; An, H.-Y.; Zhang, W.; Han, G.-X.; Zhang, G.-X.; Yang, L.-G. *Dalton Trans.* **2009**, 9807. (d) Zheng, Y.-Z.; Xue, W.; Tong, M.-L.; Chen, X.-M.; Grandjean, F.; Long, G. J. *Inorg. Chem.* **2008**, *47*, 4077.

(10) (a) Gao, E.-Q.; Liu, P.-P.; Wang, Y.-Q.; Yue, Q.; Wang, Q.-L. *Chem.—Eur. J.* **2009**, *15*, 1217. (b) Gao, E.-Q.; Wang, Z.-M.; Yan, C.-H. *Chem. Commun.* **2003**, 1748. (c) Zeng, Y.-F.; Zhao, J.-P.; Hu, B.-W.; Hu, X.; Liu, F.-C.; Ribas, J.; Ribas-Ariño, J.; Bu, X.-H. *Chem.—Eur. J.* **2007**, *13*, 9924. (d) Tian, H.; Jia, Q.-X.; Gao, E.-Q.; Wang, Q.-L. *Chem. Commun.* **2010**, *46*, 5349.

(11) (a) Feng, P. L.; Stephenson, C. J.; Amjad, A.; Ogawa, G.; del Barco, E.; Hendrickson, D. N. *Inorg. Chem.* **2010**, *49*, 1304. (b) Feng, P. L.; Beedle, C. C.; Wernsdorfer, W.; Koo, C.; Nakano, M.; Hill, S.; Hendrickson, D. N. *Inorg. Chem.* **2007**, *46*, 8126. (c) Rumberger, E. M.; Shah, S. J.; Beedle, C. C.; Zakharov, L. N.; Rheingold, A. L.; Hendrickson, D. N. *Inorg. Chem.* **2005**, *44*, 2742. (d) Stamatatos, T. C.; Abboud, K. A.; Wernsdorfer, W.; Christou, G. *Angew. Chem., Int. Ed.* **2008**, *47*, 1.

(12) (a) Liu, T.-F.; Fu, D.; Gao, S.; Zhang, Y.-Z.; Sun, H.-L.; Su, G.; Liu, Y.-J. *J. Am. Chem. Soc.* **2003**, *125*, 13976. (b) Zheng, Y.-Z.; Xue, W.; Tong, M.-L.; Chen, X.-M.; Zheng, S.-L. *Inorg. Chem.* **2008**, *47*, 11202. (c) Yang, C. I.; Tsai, Y, J.; Hung, S. P.; Tsai, H. L.; Nakano, M. *Chem. Commun.* **2010**, *46*, 5716. (d) Xu, H.-B.; Wang, B.-W.; Pan, F.; Wang, Z.-M.; Gao, S. *Angew. Chem., Int. Ed.* **2007**, *46*, 7388. (e) Zheng, Y.- Z.; Tong, M.-L.; Zhang, W.-X.; Chen, X.-M. *Angew. Chem., Int. Ed.* **2006**, *45*, 6310.

(13) (a) Thompson, L. K.; Tandon, S. S.; Lloret, F.; Cano, J.; Julve, M. *Inorg. Chem.* **1997**, *36*, 3301. (b) Liu, T.; Zhang, Y.-J.; Wang, Z.-M.; Gao, S. *Inorg. Chem.* **2006**, *45*, 2782. (c) Wang, X.-T.; Wang, X.-H.; Wang, Z.-M.; Gao, S. *Inorg. Chem.* **2009**, *48*, 1301.

(14) (a) Zeng, Y.-F.; Hu, X.; Liu, F.-C.; Bu, X.-H. *Chem. Soc. Rev.* **2009**, *38*, 469. (b) Yu, Q.; Zeng, Y.-F.; Zhao, J.-P.; Yang, Q.; Hu, B.-W.; Chang, Z.; Bu, X.-H. *Inorg. Chem.* **2010**, *49*, 4301. (c) Yang, Q.; Zhao, J.-P.; Hu, B.-W.; Zhang, X.-F.; Bu, X.-H. *Inorg. Chem.* **2010**, *49*, 3746. (d) Zeng, Y.-F.; Zhao, J.-P.; Hu, B.-W.; Hu, X.; Liu, F.-C.; Ribas, J.; Arino, J. R.; Bu, X.-H. *Chem.—Eur. J.* **2007**, *13*, 9924.

(15) (a) Escuer, A.; Vicente, R.; Mautner, F. A.; Goher, M. A. S. *Inorg. Chem.* **1997**, *36*, 1233. (b) Milios, C. J.; Prescimone, A.; Sanchez-Benitez, J.; Parsons, S.; Murrie, M.; Brechin, E. K. *Inorg. Chem.* **2006**, *45*, 7053. (c) Mondal, K. C.; Sengupta, O.; Nethaji, M.; Mukherjee, P. S. *Dalton Trans.* **2008**, *6*, 767. (d) Han, Y.-F.; Wang, T.-W.; Song, Y.; Shen, Z.; You, X.-Z. *Inorg. Chem. Commun.* **2008**, *11*, 207.

(16) (a) Chen, H.-J.; Mao, Z.-W.; Gao, S.; Chen, X.-M. *Chem. Commun.* **2001**, 2320. (b) He, Z.; Wang, Z.-M.; Gao, S.; Yan, C.-H. *Inorg. Chem.* **2006**, *45*, 6694. (c) Liu, F.-C.; Zeng, Y.-F.; Li, J.-R.; Bu, X.-H.; Zhang, H.-J.; Ribas, J. *Inorg. Chem.* **2005**, *44*, 7298.

(17) (a) Wang, Y.-Q.; Zhang, J.-Y.; Jia, Q.-X.; Gao, E.-Q.; Liu, C.-M. *Inorg. Chem.* **2009**, *48*, 789. (b) Tian, C.-Y.; Sun, W.-W.; Jia, Q.-X.; Tian, H.; Gao, E.-Q. *Dalton Trans.* **2009**, 6109. (c) Wang, Y.-Q.; Jia, Q.-X.; Wang, K.; Cheng, A.-L.; Gao, E.-Q. *Inorg. Chem.* **2010**, *49*, 1551. (d) Sun, W.-W.; Tian, C.-Y.; Jing, X.-H.; Wang, Y.-Q.; Gao, E.-Q. *Chem. Commun* **2009**, 4741. (e) Ma, Y.; Wang, Kun.; Gao, E.-Q.; Song, You. *Dalton Trans.* **2010**, *39*, 7714.

(18) (a) Ma, Y.; Zhang, J.-Y.; Cheng, A.-L.; Sun, Q.; Gao, E.-Q.; Liu, C.-M. *Inorg. Chem.* **2009**, *48*, 6142. (b) Jia, Q.-X.; Tian, H.; Zhang, J.-Y.; Gao, E.-Q. *Chem.—Eur. J.* **2011**, *17*, 1040. (c) Ma, Y.; Wen, Y.-Q.; Zhang, J.-Y.; Gao, E.-Q.; Liu, C.-M. *Dalton Trans.* **2010**, *39*, 1846. (d) Zhang, X.-M.; Wang, Y.-Q.; Wang, K.; Gao, E.-Q.; Liu, C.-M. *Chem. Commun.* **2011**, *47*, 1815.

(19) Zheng, F. K.; Wu, A. Q.; Li, Y.; Guo, G. C.; Huang, J. S. *Chin. J. Struct. Chem.* **2005**, *24*, 940.

(20) Sheldrick, G. M. *Program for Empirical Absorption Correction of Area Detector Data*; University of Göttingen: Göttingen, Germany, 1996.

(21) Sheldrick, G. M. *SHELXTL*, version 5.1.; Bruker Analytical X-ray Instruments Inc.: Madison, WI, 1998.

(22) (a) Blatov, V. A.; Shevchenko, A. P. *TOPOS 4.0*; Samara State University: Samara, Russia, 2008. (b) Reticular Chemistry Structure Resource (RCSR), http://rcsr.anu.edu.au/: O'Keeffe, M.; Peskov, M. A.; Ramsden, S. J.; Yaghi, O. M. *Accts. Chem. Res.* **2008**, *41*, 1782−1789.

(23) Ising, E. *Z. Phys.* **1925**, *31*, 253.

(24) (a) Scalapino, D. J.; Imry, Y.; Pincus, P. *Phys. Rev. B* **1975**, *11*, 2042. (b) Žumer, S. *Phys. Rev. B* **1980**, *21*, 1298.

(25) Imry, Y.; Montano, P. A.; Hone, D. *Phys. Rev. B* **1975**, *12*, 253.

(26) Coulon, C.; Clérac, R.; Lecren, L.; Wernsdorfer, W.; Miyasaka, H. *Phys. Rev. B* **2004**, *69*, 132408.

(27) Miyasaka, H.; Takayama, K.; Saitoh, A.; Furukawa, S.; Yamashita, M.; Clérac, R. *Chem.—Eur. J.* **2010**, *16*, 3656.

(28) (a) Chandra, V. R.; Ramasesha, S.; Sen, D. *Phys. Rev. B.* **2004**, *70*, 144404. (b) Vindigni, A.; Regnault, N.; Jolicoeur, T. *Phys. Rev. B.* **2004**, *70*, 134423.

(29) (a) Chikazumi, S. *Physics of Ferromagnetism*; Clarendon Press Oxford Science Publications: Oxford, U.K., 1997. (b) Miyasaka, H.; Nakata, K.; Lecren, L.; Coulon, C.; Nakazawa, Y.; Fujisaki, T.; Sugiura, K. I.; Yamashita, M.; Clérac, R. *J. Am. Chem. Soc.* **2006**, *128*, 3770.

(30) (a) Yoon, J. H.; Ryu, D. W.; Kim, H. C.; Yoon, S. W.; Suh, B. J.; Hong, C. S. *Chem.—Eur. J.* **2009**, *15*, 3661. (b) Visinescu, D.; Madalan, A. M.; Andruh, M.; Duhayon, C.; Sutter, J. P.; Ungur, L.; Heuvel, W. V.; Chibotaru, L. F. *Chem.—Eur. J.* **2009**, *15*, 11808. (c) Stamatatos, T. C.; Abboud, K. A.; Wernsdorfer, W.; Christou, G. *Inorg. Chem.* **2009**, *48*, 807. (d) Pardo, E.; Train, C.; Lescouëzec, R.; Journaux, Y.; Pasán, J.; Ruiz-Pérez, C.; Delgado, F. S.; Ruiz-Garcia, R.; Lloret, F.; Paulsen, C. *Chem. Commun.* **2010**, *46*, 2322.

(31) Mydosh, J. A. *Spin Glasses: An Experimental Introduction*; Taylor & Francis: London, U.K., 1993.

(32) Tsurkan, V.; Hemberger, J.; Klemm, M.; Klimm, S.; Loidl, A.; Horn, S.; Tidecks, R. *J. Appl. Phys.* **2001**, *90*, 4639.

(33) (a) Cole, K.-S.; Cole, R.-H. *J. Chem. Phys.* **1941**, *9*, 341. (b) Boettcher, C. J. F. *Theory of Electric Polarisation*; Elsevier: Amsterdam, The Netherlands, 1952. (c) Aubin, S. M.; Sun, Z.; Pardi, L.; Krzysteck, J.; Folting, K.; Brunel, L.-J.; Rheingold, A. L.; Christou, G.; Hendrickson, D. N. *Inorg. Chem.* **1999**, *38*, 5329.

(34) Coulon, C.; Clérac, R.; Wernsdorfer, W.; Colin, T.; Miyasaka, H. *Phys. Rev. Lett.* **2009**, *102*, 167204.

(35) Levin, E. M.; Pecharsky, V. K.; Gschneider, K. A., Jr. *J. Appl. Phys.* **2001**, *90*, 6255.

(36) Coulon, C.; Clérac, R.; Wernsdorfer, W.; Colin, T.; Saitoh, A.; Motokawa, N.; Miyasaka, H. *Phys. Rev. B* **2007**, *76*, 214422.

(37) Borrás-Almenar, J. J.; Clemente-Juan, J. M.; Coronado, E.; Tsukerblat, B. S. *Inorg. Chem.* **1999**, *38*, 6081.

(38) (a) Abu-Youssef, M. A. M.; Escuer, A.; Gatteschi, D.; Goher, M. A. S.; Mautner, F. A.; Vicente, R. *Inorg. Chem.* **1999**, *38*, 5716. (b) Abu-Youssef, M. A. M.; Escuer, A.; Vicente, R.; Mautner, F. A.; Öhrstrom, L.; Goher, M. A. S. *Polyhedron* **2005**, *24*, 557. (c) Bitschnau, B.; Egger, A.; Escuer, A.; Mautner, F. A.; Sodin, B.; Vicente, R. *Inorg. Chem.* **2006**, *45*, 868.

(39) (a) Borrás-Almenar, J. J.; Coronado, E.; Gallart, J. C.; Georges, R.; Gómez-Garcia, C. J. *J. Magn. Magn. Mater.* **1992**, *104 −107*, 835. (b) Otsuka, H. *Phys. Rev. B* **1995**, *51*, 305. (c) Nakamura, T.; Kubo, K. *Phys. Rev. B* **1996**, *53*, 6393. (d) Nakamura, T.; Takada, S. *Phys. Rev. Lett. A* **1997**, *225*, 315. (e) Georges, R.; Borrás-Almenar, J. J.; Coronado, E.; Curély, J.; Drillon, M. in ref.,[3b] Vol. *I*, p22. (f) Cheng, X.-N.; Zhang, W.-X.; Zheng, Y.-Z.; Chen, X.-M. *Chem. Commun.* **2006**, 3603. (g) Gutschke, S. O. H.; Price, D. J.; Powell, A. K.; Wood, P. T. *Angew. Chem., Int. Ed.* **2001**, *40*, 1920. (h) Stephenson, J. *Can. J. Phys.* **1970**, *48*, 1724.

(40) (a) Greedan, J. E. *J. Mater. Chem.* **2001**, *11*, 37. (b) Richter, J.; Schulenburg, J.; Honecker, A. *Lect. Notes Phys.* **2004**, *645*, 85. (c) Gao, E.-Q.; Liu, N.; Cheng, A.-L.; Gao, Song. *Chem. Commun.* **2007**, 2470.